

# **NGC 4593**

Untertitel (falls nötig)

Vorname Nachname

Universität XYZ

Betreuer: Dr. XYZ

July 12, 2025

## **Abstract**

Abstract

# Contents

<b>1</b>	<b>Introduction</b>	<b>5</b>
<b>2</b>	<b>Scientific Background</b>	<b>6</b>
2.1	Active Galactic Nuclei . . . . .	6
2.1.1	Structure and spectral Features of an AGN . . . . .	6
2.1.2	Classification . . . . .	9
2.1.3	Unification Model . . . . .	11
2.1.4	Variability . . . . .	12
2.2	Reverberation Mapping . . . . .	12
2.2.1	Principle . . . . .	12
2.2.2	Transferfunction . . . . .	12
2.2.3	Cross-Correlation Function . . . . .	12
2.2.4	Black-Hole Mass . . . . .	12
2.3	Bowen Fluorescence . . . . .	12
<b>3</b>	<b>Campaign and Analysis</b>	<b>13</b>
3.1	NGC4593 . . . . .	13
3.2	2016 Campaign by E. M. Cackett . . . . .	13
3.3	Intercalibration . . . . .	14
<b>4</b>	<b>Reverberation Analysis of NGC4593</b>	<b>15</b>
4.1	AVG- and RMS-Spectrum . . . . .	15
4.2	Lightcurves . . . . .	15
4.2.1	Continua . . . . .	15
4.2.2	Emission Lines . . . . .	15
4.3	Line Profiles . . . . .	15
4.4	Cross-Correlation Function . . . . .	15
4.5	Time Lag and BH Masses . . . . .	15
4.6	Bowen Fluorescence . . . . .	15



# List of Figures

2.1	Different components of an AGN. Adapted from Mo, Bosch, and White (2010) Figure 14.3. . . . .	7
2.2	Unification model of an AGN (Fermi Gamma-ray Space Telescope 2025). . . . .	11
3.1	A DSS image of NGC4593. . . . .	13

# List of Tables

3.1 Overview of STIS Grating Characteristics (Space Telescope Science  
Institute 2025) . . . . . 14

# 1. Introduction

## 2. Scientific Background

### 2.1 Active Galactic Nuclei

What are Active Galactic Nuclei (AGN)? An Active Galactic Nucleus (AGN) refers to the central region of a galaxy that is exceptionally bright and energetic. These regions are among the most luminous objects in the universe, with bolometric luminosities ranging from  $10^{41}$  to  $10^{48}$  erg s<sup>-1</sup>, outshining entire galaxies by several orders of magnitude (Bradley M. Peterson 1997). Its emission spans the entire electromagnetic spectrum and is powered by the accretion of matter onto the supermassive black hole (SMBH) in the center of the AGN. The most common model for this accretion is a hot, rotating accretion disk around the SMBH, which is responsible for most of the observed radiation (Shakura and Sunyaev 1973).

To provide a basic understanding of the structure and physical processes within AGN, the following sections outline their key components, introduce the unification model that connects various AGN types, and summarize common classification schemes. Particular emphasis is placed on AGN variability, which plays a central role in the reverberation mapping analysis conducted in this thesis.

#### 2.1.1 Structure and spectral Features of an AGN

The structure of an AGN consists of several components, which are illustrated schematically in Figure 2.1. These include a central supermassive black hole (SMBH), an accretion disk that feeds the SMBH, a surrounding dusty torus, and ionized gas regions known as the broad-line region (BLR) and narrow-line region (NLR). In some AGNs, powerful relativistic jets are launched perpendicular to the accretion disk. However, these jets will not be discussed further in this section, as they are not relevant to the scope of this thesis.



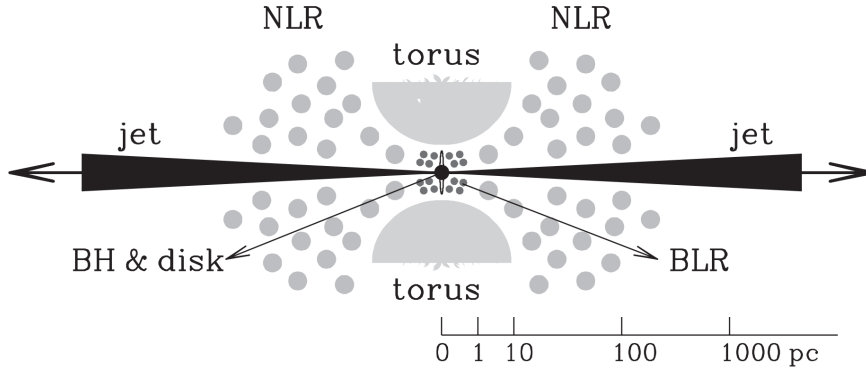


Figure 2.1: Different components of an AGN. Adapted from Mo, Bosch, and White (2010) Figure 14.3.

### Supermassive Black Hole and Accretion Disk

The center of an AGN is occupied by a supermassive black hole (SMBH), with masses typically ranging from  $10^6 M_{\odot}$  to more than  $10^{10} M_{\odot}$ . While the SMBH itself does not emit radiation, it dominates the gravitational potential in the innermost regions and acts as the central engine for all observed AGN phenomena. The matter from the surrounding accretion disk slowly spirals inward toward the SMBH due to angular momentum transport driven by viscosity inside the disk. The accretion disk itself is a geometrically thin and optically thick structure composed of ionized gas in differential rotation around the SMBH (Shakura and Sunyaev 1973). The disk's composition is primarily ionized hydrogen and helium, with traces of heavier elements (Netzer 2013). It extends from the innermost stable circular orbit (ISCO) near the event horizon out to distances of several light-days. The radial extent of the disk is relatively small on galactic scales, typically ranging from a few light-hours to a few light-days, corresponding to about  $10^{-3}$  to  $10^{-2}$  pc (Netzer 2013; Hickox and Alexander 2018).

During the accretion process, gravitational potential energy is converted into heat, causing the disk to reach very high temperatures. As a result, a significant fraction of the gravitational energy of the matter is transformed into thermal radiation, which accounts for the enormous luminosity observed in AGNs and heats the accretion disk depending on the size of the SMBH. While the maximum effective temperature for an accretion disk around a SMBH with  $M = 10^8 M_{\odot}$  is on the order of several  $\times 10^5$  K, leading to UV emission and optical emission. In comparison, disks around stellar-mass black holes reach much higher temperatures (up to a few  $\times 10^6$  K), emitting mostly in X-rays (Netzer 2013). Due to the temperature gradient with hotter regions in the inner disk, the emitted spectrum can not be described as

a single blackbody. Instead, it results from combination of many blackbody like components at different temperatures, often referred to as a multi-color blackbody. This creates a broad optical-UV continuum that cannot be fully described by simple blackbody radiation. In addition, processes like electron scattering and relativistic effects near the black hole further modify the shape of the spectrum (Netzer 2013). The ionizing photons, emitted by the continuum, play a crucial role for other spectral features. They interact with the surrounding gas clouds near the nucleus, causing photo-ionization followed by recombination. This process leads to different kinds of strong emission lines, which are characteristic features of AGN spectra (Osterbrock 1989).

### **Broad-Line and Narrow-Line Region**

Outside the accretion disk lies a distribution of gas clouds photo-ionized by the energetic photons of the accretion disk continuum. The innermost of these clouds is the broad-line region (BLR), located at distances of a few light-days to light-weeks from the central SMBH. The BLR consists of dense gas clouds moving at high velocities of several thousand kilometers per second due to the strong gravitational influence of the black hole (Netzer 2013). These velocities lead to a significant Doppler broadening of permitted emission lines and line widths of several thousand km/s. As described earlier, the BLR is primarily photo-ionized by the continuum radiation emitted from the accretion disk. As a result, the line emission from this region is strongly correlated with the continuum emission, which is particularly important for reverberation mapping, which will be discussed later in Section 2.2.

The exact geometry of the BLR remains uncertain, with models ranging from a spherical distribution of clouds to a flattened disk-like structure. (Netzer 2013). Broad emission lines appear in permitted transitions such as  $H\alpha$ ,  $H\beta$  and  $Ly\alpha$ . (Bradley M. Peterson 1997)

Further out lies the narrow-line region (NLR). The gas in this region moves at much lower velocities, resulting in narrow emission lines with widths typically below 1000, km/s. In contrast to the BLR, the NLR allows both permitted and forbidden transitions. The Forbidden Lines, such as  $[O,III]\lambda 5007$ , arise due to collisional excitation and can only form in low-density environments with electron densities around  $10^2 - 10^6 \text{ cm}^{-3}$  (Osterbrock 1989).

## **Dusty Torus**

Surrounding the accretion disk and broad-line region is the dusty torus, a geometrically thick and optically dense structure composed of gas and dust. It extends from the sublimation radius, where dust can survive the intense radiation of the accretion disk, out to scales of a few parsecs. The torus likely has a clumpy distribution and plays a crucial role in the unified model of AGNs which will be discussed in a later section (Netzer 2013; Hickox and Alexander 2018). The dust in the torus absorbs a significant fraction of the UV and optical radiation emitted by the accretion disk and re-emits it thermally in the infrared. As a result, AGNs typically exhibit strong infrared emission, with the peak wavelength depending on the dust temperature. This reprocessed radiation provides an important observational signature and can be used to trace obscured AGN activity, especially in AGNs where the central region is hidden from direct view (Netzer 2013).

### **2.1.2 Classification**

As previously implied, AGN emit across the entire electromagnetic spectrum, with their emission characteristics strongly depending on their internal structure. Consequently, each AGN exhibits a unique spectral signature, based on which they have historically been classified.

These classifications are based on the differences in luminosity, emission-line profiles, and radio properties. Broadly, AGNs can be grouped into Seyfert galaxies, quasars, and radio galaxies. Seyfert galaxies are further subdivided based on the width of their optical emission lines and their radio characteristics. Seyfert 1 galaxies exhibit both broad and narrow emission lines, where Seyfert 2 galaxies show only narrow emission lines. Besides those main classes there are additional subclasses including narrow-line Seyfert 1 galaxies (NLS1s), low-ionization nuclear emission-line regions (LINERs), and jet-dominated sources such as BL Lac objects or blazars (Antonucci 1993; Urry and Padovani 1995).

### **Seyfert Galaxies**

Seyfert galaxies are named after Carl K. Seyfert, who in 1943 observed spiral galaxies characterized by exceptionally bright nuclei and prominent broad emission lines in their optical spectra (Seyfert 1943). For that they represent a class of AGN with bright nuclei and strong emission lines. Today, they are classified primarily based on the presence and width of permitted and forbidden low- and high-ionized emission lines.

Seyfert 1 galaxies, of which NGC 4593 is an example, show both broad and narrow emission lines in their optical spectra. The broad lines, such as  $H_\alpha$  and  $H_\beta$ , have a full width at half maximum (FWHM) of typically several thousand kilometers per second and arise from the high-velocity BLR. In contrast, narrow lines, including prominent forbidden transitions like [O III]  $\lambda 5007$  or [N II]  $\lambda 6584$ , originate from the lower-velocity NLR (Osterbrock 1989; Bradley M. Peterson 1997).

The presence of both components in the spectrum allows for a clear classification as a Seyfert 1 galaxy, which is the case for NGC4593. More to NGC4593 in section 3.1.

In comparison, Seyfert 2 galaxies lack these broad components in their optical spectra, likely due to orientation-dependent obscuration by circumnuclear material. This distinction is central to the Unified Model of AGN, which attributes observed differences between Seyfert types primarily to the viewing angle rather than intrinsic differences in structure and will be deepened in section 2.1.3 (Antonucci 1993; Urry and Padovani 1995).

Another notable subclass are the so-called narrow-line Seyfert 1 galaxies (NLS1s). Despite their classification as Seyfert 1, the broad permitted lines in their spectra exhibit unusually small widths, with  $\text{FWHM} < 2000 \text{ km s}^{-1}$ . They often show strong Fe II emission complexes and steep soft X-ray spectra. NLS1s are thought to have low-mass black holes accreting at high Eddington rates, suggesting they may represent a young evolutionary phase of AGN activity (Osterbrock and Pogge 1985; Netzer 2013).

## Others

Next to Seyfert galaxies, there are several other classes of AGN. Quasars, short for quasi-stellar radio sources, are even more luminous than Seyfert galaxies and are typically found at higher redshifts. While the host galaxies of Seyfert galaxies are still observable, quasars completely outshine their host galaxies. Since quasars show similar emission characteristics to Seyfert galaxies, the modern distinction is based mainly on luminosity: quasars are classified as high-luminosity AGNs, while Seyferts represent the lower-luminosity end (Netzer 2013).

Radio galaxies are defining another AGN class. They are characterized by their strong radio emission and prominent jets, often associated with elliptical host galaxies. When their jets are aligned close to our line of sight, they are observed as blazars or BL Lac objects, which exhibit rapid variability and featureless optical spectra due to relativistic beaming (Netzer 2013).

Finally, LINERs are low-luminosity AGNs with spectra dominated by low-ionization

emission lines. The physical origin of their ionization mechanism is still debated, and in some cases, they may not be powered by accretion at all (Netzer 2013).

### 2.1.3 Unification Model

Figure 2.2 shows the unification model of an AGN. As illustrated an AGN is powered by a supermassive black hole surrounded by several distinct regions. Closest to the black hole is the accretion disc, whose hot, optically thick gas emits the thermal “Big Blue Bump” in the optical/UV bands (Bradley M. Peterson 1997). Encircling the disc is the Broad-Line Region (BLR), a compact area of dense clouds orbiting at thousands of kilometers per second, which produces the broad emission lines. Outside the BLR lies the dusty torus, a toroidal structure of cooler gas and dust that can obscure the inner regions when viewed edge-on (Antonucci 1993). Beyond the torus, the more extended Narrow-Line Region (NLR) emits narrower lines from slower gas at distances of hundreds of parsecs. In radio-loud AGN, powerful relativistic jets emerge perpendicular to the disc plane, accelerating particles to near-light speeds and generating strong radio emission (Urry and Padovani 1995).

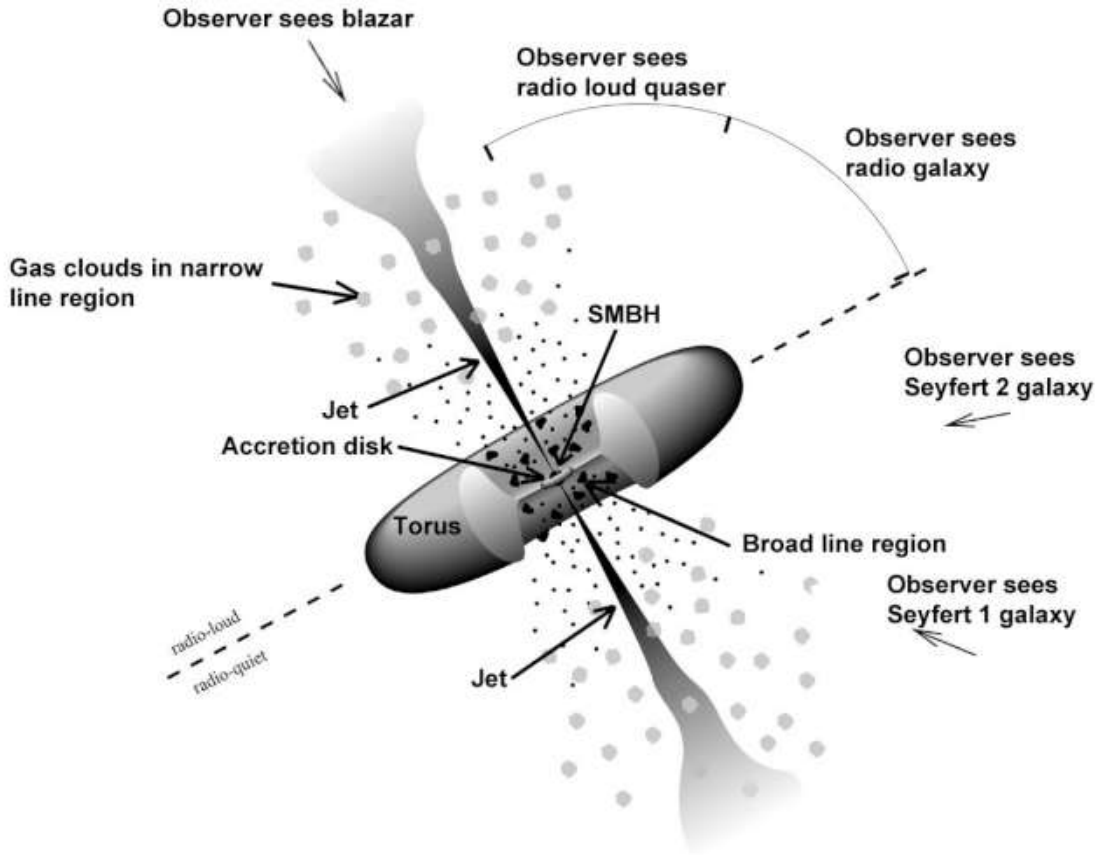


Figure 2.2: Unification model of an AGN (Fermi Gamma-ray Space Telescope 2025).

#### **2.1.4 Variability**

### **2.2 Reverberation Mapping**

#### **2.2.1 Principle**

The main focus of this work was to perform a classic reverberation analysis of NGC 4593, with a focus on the broad line region (BLR) and its geometry around the central supermassive black hole (SMBH).

This type of analysis aims to measure the time lag  $\tau$  between the variable continuum and the emission line response, in order to determine the spatial scale and structure of the BLR. By observing these variations over time and analyzing the delayed response of the broad lines, it is possible to learn more about the geometry and dynamics of the BLR and to estimate the mass of the SMBH.

Reverberation mapping (RM) is based on the strong correlation between a variable continuum emission  $C(t)$  and the emission line flux  $L(\nu, t)$  (Horne et al. 2021). This correlation originates from the photoionization of gas clouds in the BLR by the central continuum source. As the continuum changes, the emission lines react in a similar way, but with a time delay  $\tau$ , because of the distance between the central source and the BLR. This delay corresponds to the time it takes for light to travel from the central source to the BLR.

#### **2.2.2 Transferfunction**

#### **2.2.3 Cross-Correlation Function**

#### **2.2.4 Black-Hole Mass**

### **2.3 Bowen Fluorescence**

## 3. Campaign and Analysis

The Analysis of this campaign bases of the observation campaign of NGC4593 in 2016 by Edward M. Cackett (Edward M Cackett et al. 2018). The observations took place between the 12th of July and the 6th of August with 26 successful observations and was performed with the Hubble Space Telescope (HST) using the Space Telescope Imaging Spectrograph (STIS). The following section will cover important properties of NGC4593 and the 2016 campaign.

### 3.1 NGC4593

NGC4593 is an active galactic nuclei (AGN), classified as an Seyfert 1 Galaxy with a Sb D morphology. It is located at RA = 12:39:39.44, DEC = -05:20:39.03 (2000) and has a of  $z = 0.0083 \pm 0.0005$  This correspond to a distance of about 35.6 MPc (SIMBAD 2025)based on the  $\Lambda$ CDM-Model.

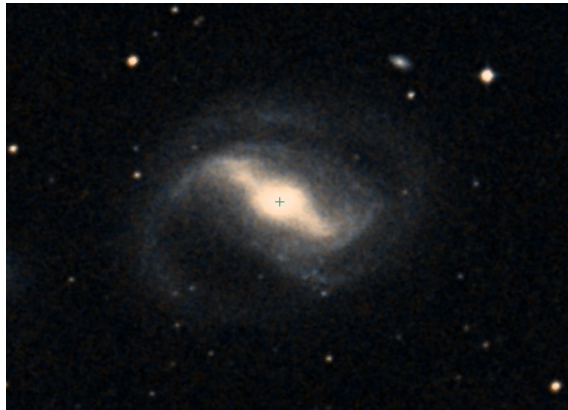


Figure 3.1: A DSS image of NGC4593.

### 3.2 2016 Campaign by E. M. Cackett

E. M. Cackett's campaign was designed to study wavelength dependent continuum lags. Therefore, the STIS instrument on the Hubble Space Telescope was used

with low-resolution gratings to measure a broad range of wavelengths. In each observation, spectra were taken using three different gratings: G140L, G430L, and G750L. These were used together with the  $52'' \times 0.2''$  slit.

The characteristics of the STIS gratings used in this analysis are summarized in Table 3.1.

Table 3.1: Overview of STIS Grating Characteristics (Space Telescope Science Institute 2025)

<b>Grating</b>	<b>Range [Å]</b>	<b>Exp. Time [s]</b>	<b>Res. Power</b>	<b>Dispersion [Å/pixel]</b>
G140L	1119–1715	1234	$\sim 1000$	0.6
G430L	2888–5697	298	$\sim 500 - 1000$	2.73
G750L	5245–10233	288	$\sim 500 - 1000$	4.92

### 3.3 Intercalibration



## 4. Reverberation Analysis of NGC4593

### 4.1 AVG- and RMS-Spectrum

### 4.2 Lightcurves

#### 4.2.1 Continua

#### 4.2.2 Emission Lines

### 4.3 Line Profiles

### 4.4 Cross-Correlation Function

### 4.5 Time Lag and BH Masses

### 4.6 Bowen Fluorescence

## 5. Discussion

# Bibliography

- Antonucci, Robert (1993). “Unified models for active galactic nuclei and quasars”. In: *Annual Review of Astronomy and Astrophysics* 31, pp. 473–521. DOI: 10.1146/annurev.aa.31.090193.002353.
- Cackett, Edward M et al. (2018). “Accretion disk reverberation with Hubble space telescope observations of NGC 4593: evidence for diffuse continuum lags”. In: *The Astrophysical Journal* 857.1, p. 53.
- Fermi Gamma-ray Space Telescope (2025). *Figure 1: Spectral Energy Distribution of an AGN*. URL: <https://fermi.gsfc.nasa.gov/science/etev/agn/figure1.jpg> (visited on 06/19/2025).
- Hickox, Ryan C. and David M. Alexander (2018). “Obscured Active Galactic Nuclei”. In: *Annual Review of Astronomy and Astrophysics* 56, pp. 625–671. DOI: 10.1146/annurev-astro-081817-051719. arXiv: 1806.04680 [astro-ph.GA].
- Horne, Keith et al. (2021). “Space telescope and optical reverberation mapping project. IX. velocity–delay maps for broad emission lines in NGC 5548”. In: *The Astrophysical Journal* 907.2, p. 76.
- Mo, Houjun, Frank van den Bosch, and Simon White (2010). *Galaxy Formation and Evolution*. Cambridge University Press. ISBN: 9780521857932.
- Netzer, Hagai (2013). *The Physics and Evolution of Active Galactic Nuclei*. Cambridge: Cambridge University Press.
- Osterbrock, Donald E. (1989). *Astrophysics of Gaseous Nebulae and Active Galactic Nuclei*. Mill Valley, California: University Science Books. ISBN: 9780935702111.
- Osterbrock, Donald E. and Richard W. Pogge (1985). “The spectra of narrow-line Seyfert 1 galaxies”. In: *The Astrophysical Journal* 297, pp. 166–176. DOI: 10.1086/163513.
- Peterson, Bradley M. (1997). *An Introduction to Active Galactic Nuclei*. Cambridge University Press. ISBN: 9780521473484.
- Seyfert, Carl K. (1943). “Nuclear Emission in Spiral Nebulae”. In: *The Astrophysical Journal* 97, pp. 28–40. DOI: 10.1086/144488.

- Shakura, N. I. and R. A. Sunyaev (1973). “Black holes in binary systems. Observational appearance”. In: *Astronomy and Astrophysics* 24, pp. 337–355.
- SIMBAD (2025). *NGC4593*. URL: <https://simbad.u-strasbg.fr/simbad/sim-id?Ident=NGC4593> (visited on 06/10/2025).
- Space Telescope Science Institute (2025). *STIS Instrument Handbook: Gratings*. URL: <https://hst-docs.stsci.edu/stisihb/chapter-13-spectroscopic-reference-material/13-3-gratings> (visited on 05/12/2025).
- Urry, C. Megan and Paolo Padovani (1995). “Unified Schemes for Radio-Loud Active Galactic Nuclei”. In: *Publications of the Astronomical Society of the Pacific* 107.715, pp. 803–845. DOI: 10.1086/133630.